Acta Crystallographica Section B
Structural Science
ISSN 0108-7681

Low-temperature structure of V_6O_{13}

Jonas Höwing,* Torbjörn Gustafsson and John O. Thomas

Department of Materials Chemistry, The Ångström Laboratory, Uppsala University, Box 538, SE-751 21 Uppsala, Sweden

Correspondence e-mail: howing@mkem.uu.se

Received 12 August 2003
Accepted 17 October 2003

The structure of the transition metal oxide V_6O_{13}, a potential cathode material in lithium-polymer batteries, has been studied at 95 K using single-crystal X-ray diffraction (XRD). A phase transition has been determined by differential scanning calorimetry (DSC) measurements to occur at 153 K, with a heat of transition of -1.98 kJ mol^{-1}. In this low-temperature phase, the V and O atoms move by up to 0.21 Å out of the mirror plane they occupy in the room-temperature structure. It is concluded that the earlier reported space group $P2_1/a$ [Kawada *et al.* (1978). *Acta Cryst.* B**34**, 1037–1039] is incorrect and that a more appropriate choice of space group is *Pc*.

1. Introduction

Lithium-ion batteries are today the most commonly used power source for portable electronics, such as cellular phones and laptop computers. They comprise a lithium transition-metal oxide (TMO) cathode, a Li-ion conducting polymer or organic liquid electrolyte and a graphite anode. When the battery is charged, lithium is extracted from the TMO cathode and intercalated into the graphite. The voltage range for a typical commercial battery using $LiCoO_2$ as the cathode material is 3.75–4.2 V. Other cathode materials under extensive research include doped $LiCoO_2$, such as $Li(Mg,Ni,Co)O_2$ (Chang *et al.*, 2000) and $LiNi_xCo_{1-x}O_2$ (Gover *et al.*, 2000), $LiMn_2O_4$ (Thackeray *et al.*, 1983) and $Li(Al,Ni)O_2$ (Ohzuku *et al.*, 1999).

A transition-metal oxide which has long been studied as a potential cathode material for a lithium-polymer battery (involving a metallic lithium anode) is V_6O_{13}. The electrode reactions in such a cell are

$$\text{Anode reaction :} \quad x\text{Li} \rightarrow x\text{Li}^+ + xe^-$$

$$\text{Cathode reaction :} \quad \text{V}_6\text{O}_{13} + x\text{Li}^+ + xe^- \rightarrow \text{Li}_x\text{V}_6\text{O}_{13}$$

$$\text{Cell reaction :} \quad x\text{Li} + \text{V}_6\text{O}_{13} \Leftrightarrow \text{Li}_x\text{V}_6\text{O}_{13}.$$

V_6O_{13} can host as many as six Li atoms per formula unit and the insertion process is fully reversible. In practise, this gives a capacity of *ca* 310 mAh g^{-1} compared with *ca* 150 mAh g^{-1} for $LiCoO_2$, where only slightly more than half of the lithium content can be utilized. The structure of pure V_6O_{13} comprises edge- and corner-sharing VO_6 octahedra arranged in alternating single and double layers with corner sharing between the layers, in space group $C2/m$ (Wilhelmi *et al.*, 1971). During discharge (lithiation) V_6O_{13} passes through a series of phase transitions. Single-crystal XRD studies have already been

Table 1
Experimental details.

	Stoe data	Bruker data
Crystal data		
Chemical formula	V_6O_{13}	V_6O_{13}
M_r	513.64	513.64
Cell setting, space group	Monoclinic, *Pc*	Monoclinic, *Pc*
a, *b*, *c* (Å)	10.0605 (4), 3.7108 (3), 11.9633 (6)	10.0543 (1), 3.7080 (1), 11.9554 (1)
β (°)	100.927 (4)	100.914 (1)
V (Å^3)	438.52 (5)	437.65 (1)
Z	2	2
D_x (Mg m^{-3})	3.890	3.896
Radiation type	Mo $K\alpha$	Mo $K\alpha$
No. of reflections for cell parameters	70	4122
θ range (°)	27.9–37.6	3.5–49.4
μ (mm^{-1})	6.06	6.23
Temperature (K)	95 (1)	95 (2)
Crystal form, colour	Brick, black	Brick, black
Crystal size (mm)	0.21 × 0.10 × 0.10	0.12 × 0.07 × 0.05
Data collection		
Diffractometer	Stoe four-circle	CCD area detector
Data collection method	$\omega/2\theta$ scans	ω scans
Absorption correction	Integration	Integration
T_{min}	0.499	0.580
T_{max}	0.609	0.775
No. of measured, independent and observed reflections	9436, 4604, 9436	26 501, 8245, 26 501
Criterion for observed reflections	$I_{net} > -15.0\sigma(I_{net})$	$I > -15\sigma(I)$
R_{int}	0.016	0.058
θ_{max} (°)	50.0	49.6
Range of *h*, *k*, *l*	$-21 \Rightarrow h \Rightarrow 21$ $-3 \Rightarrow k \Rightarrow 8$ $-25 \Rightarrow l \Rightarrow 25$	$-21 \Rightarrow h \Rightarrow 21$ $-7 \Rightarrow k \Rightarrow 6$ $-25 \Rightarrow l \Rightarrow 24$
No. and frequency of standard reflections	6 every 240 min	Not measured
Intensity decay (%)	1.7	N/A
Refinement		
Refinement on	F^2	F^2
$R[F^2 > 2\sigma(F^2)]$, $wR(F^2)$, S	0.034, 0.058, 2.60	0.078, 0.083, 0.58
No. of reflections	9436	26501
No. of parameters	191	191
H-atom treatment	No H atoms present	No H atoms present
Weighting scheme	Based on measured s.u.'s $w = 1/\sigma^2(I)$	Based on measured s.u.'s $w = 1/\sigma^2(I)$
$(\Delta/\sigma)_{max}$	0.027	0.023
$\Delta\rho_{max}$, $\Delta\rho_{min}$ (e Å^{-3})	2.26, −1.80	4.46, −4.75
Extinction method	B-C type 1 Gaussian isotropic	B-C type 1 Gaussian isotropic
Extinction coefficient	2566 (51)	683 (5)

Computer programs used: *DIF4* (Stoe & Cie, 1988), *LATCON* (Lundgren, 1983), *SAINT+* (Bruker, 200), *STOEDATRED*, *LSQLIN* and *ABSSTOE* (Lundgren, 1983), *JANA*2000 (Petříček & Dušek, 2000), *DUPALS* (Lundgren, 1983), *Diamond* Version 2.1c (Bergerhoff, 1996), *DISTAN* (Lundgren, 1983).

carried out on the structures of $Li_2V_6O_{13}$ and $Li_3V_6O_{13}$ (Bergström *et al.*, 1998*a*,*b*) and the superlattices of $Li_{2/3}V_6O_{13}$ and $Li_1V_6O_{13}$ (Björk *et al.*, 2001). V_6O_{13} has been reported to undergo a semiconductor–semiconductor phase transition at *ca* 150 K [156 (Kachi *et al.*, 1963), 147 (Saeki *et al.*, 1973) and 150 K (Dernier, 1974)]. This low-temperature structure was first solved in 1974 by Dernier in the non-centrosymmetric space group *C*2, and later by Kawada *et al.* (1978) in the centrosymmetric space group $P2_1/a$.

2. Experimental

Single crystals of V_6O_{13} were grown using a CVT (Chemical Vapour Transport) method previously reported by Saeki *et al.* (1973). The starting materials were phase-pure V_6O_{13} powder and the transport agent $TeCl_4$ (Merck, *as received*), mixed in the mass ratio 20:1. Two single-crystal diffraction experiments were performed, one on a Stoe & Cie Stadi-4 four-circle diffractometer and one on a Bruker SMART APEX system with a CCD detector. The latter experiment was carried out to look for the possible formation of a superlattice structure and to ensure that the result derived from the Stoe diffractometer data was reproducible and not an isolated observation. Mo $K\bar{\alpha}$ radiation was used in both cases. The cooling equipment used in both diffraction experiments was an Oxford Cryosystems 600 Series Cryostream Cooler using liquid nitrogen. The temperature variation of the Cryostream was 0.1 K on the Stoe diffractometer and 1 K on the Bruker diffractometer; the difference arising because of a problem with the isolation of the Cryostream system. The temperature variation at the crystal is at worst ±3 K for high χ-angle data on the Stoe diffractometer, where air can be dragged down the glass needle.

2.1. DSC measurements

DSC (Differential Scanning Calorimetry) measurements were performed on V_6O_{13} single crystals using a Mettler DSC 30 calorimeter; single crystals (12.49 mg) were placed in a standard 40 μl Al pan. The dimensions of the crystals were between 0.05 and 0.25 mm. An empty pan was used as a reference. The heating rate was set at 5 K min^{-1} and the temperature program was 303 ⇒ 113 ⇒ 303 K.

2.2. Stoe four-circle diffractometer data

Prior to cooling the crystal to below the phase transition temperature (*ca* 150 K), a complete dataset was collected at 160 K. A structure refinement based on this dataset showed that the crystal was of excellent quality. Data were then collected at 95 K. When the atoms move out of the mirror

plane they occupy at room temperature, the *C*-centring is destroyed and reflections of the type $h + k \neq 2n$ appear in the diffraction pattern. Three reflections which are systematically absent for *C*-centring were therefore monitored continuously during the cooling. Earlier studies reported problems with crystals shattering during the phase transition (Saeki *et al.*, 1973). To avoid this, the cooling rate was reduced to 0.1 K min^{-1} from 160 K down to 140 K, and the temperature kept constant for 2 h after the first sign of the phase transition taking place. The $h + k \neq 2n$ reflections were quite weak and broad. During the data collection they were therefore measured using a scan-step of 0.01° in ω, a minimum of 100 steps, and a measuring time varying from 0.3 to 2.0 s per step. Reflections with $h + k = 2n$ were measured with a scan step of 0.01° in ω with a minimum of 70 steps and a measuring time varying 0.3 to 3.0 s per step. Standard reflections were monitored over the 690 h required for the data collection and showed a systematic intensity decay of 1.7%. The ranges were $3 < 2\theta < 35°$ for $-9 \leq h \leq 9$, $-3 \leq k \leq 3$, $-8 \leq l \leq 8$; $35 < 2\theta < 100°$ for $-25 \leq h \leq 25$, $0 \leq k \leq 8$, $-21 \leq l \leq 21$. For further details, see Table 1. The data was corrected for background (Lehmann & Larsen, 1974); intensities and the corresponding standard deviations were corrected for time variations according to McCandlish *et al.* (1975). The cell parameters were refined using 70 high-angle reflections centred using Mo $K\alpha_1$ radiation. The reflections were handpicked to ensure that they were sufficiently strong and that the $K\alpha_1$ and $K\alpha_2$ components could be separated. A numerical absorption correction was applied. Data reduction was performed using the *DUPALS* program package (Lundgren, 1983).

2.3. Bruker SMART CCD diffractometer data

A new crystal was used for this experiment and data were again collected at 95 K. Close to the phase transition temperature the procedure followed was as described above. The measurements were made using 0.2° ω scans with 10 s exposure time at low angles (detector at $2\theta = 28°$) and 20 s exposure time at high angles (detector set at $2\theta = 72°$). The data collection took 185 h. The resolution used was 512 × 512 pixels. Integration of the frames, space group determination and numerical absorption correction were performed using the *SAINT*+ program package (Bruker, 2001); cell parameters were refined using 4122 reflections.

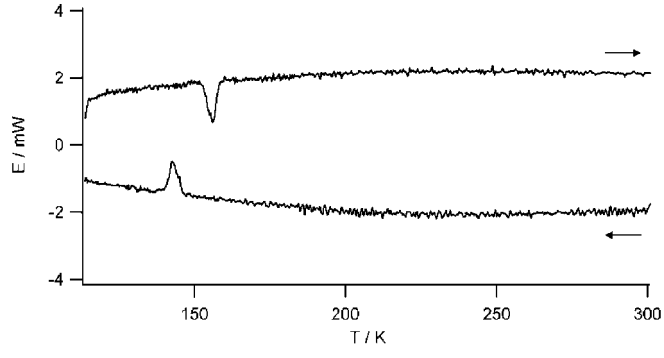

Figure 1
DSC curve for V_6O_{13} single crystals with dimensions between 0.05 and 0.25 mm. Heating rate: 5 K min^{-1}.

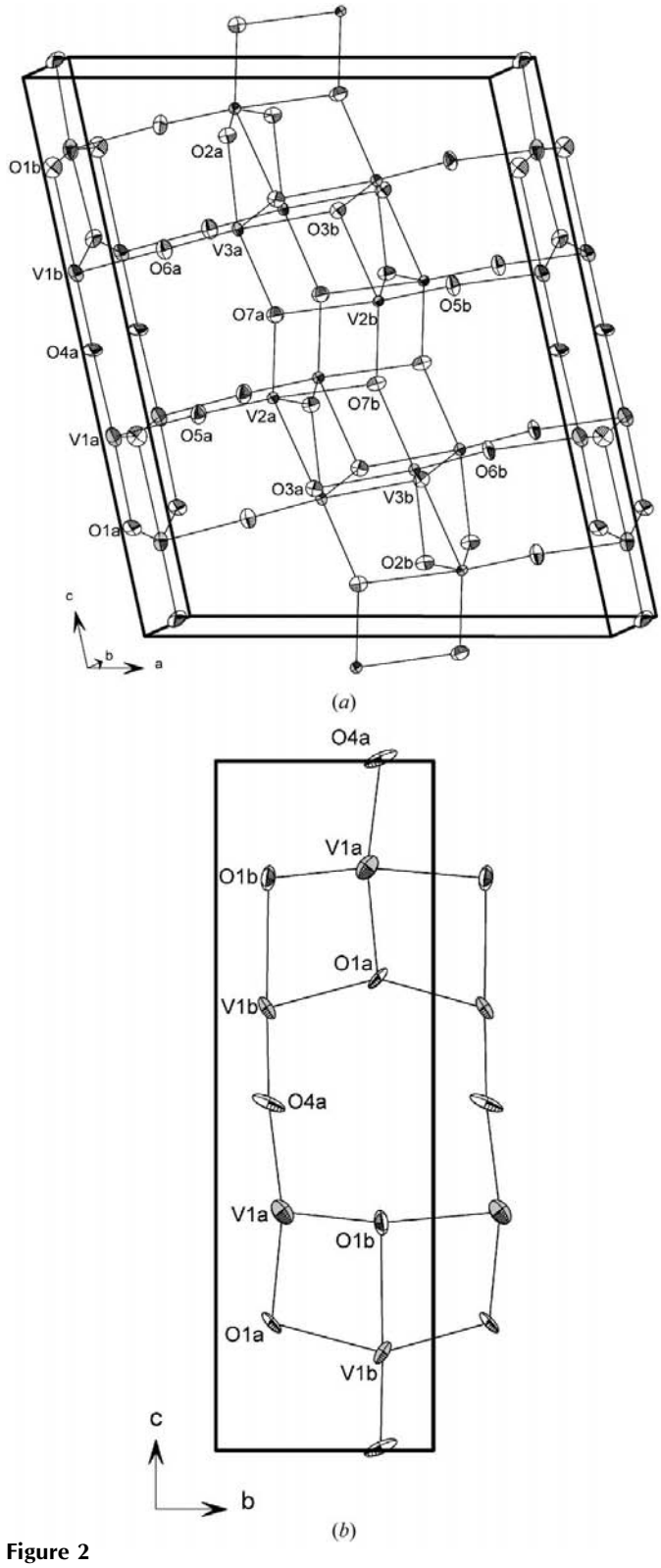

Figure 2
(*a*) The low-temperature structure of V_6O_{13} and (*b*) the single layer viewed along the *a*-axis. Displacement ellipsoids are drawn at the 95% probability level.

Table 2
Selected geometric parameters for the Stoe data (Å).

V1*a*—O1*a*	1.9363 (12)	V2*b*—O7*a*	2.2589 (14)
V1*a*—O4*a*	1.8996 (13)	V2*b*—O2*b*^{iv}	1.912 (2)
V1*a*—O5*a*	1.9708 (13)	V2*b*—O2*b*^{v}	1.920 (2)
V1*a*—O1*b*^{i}	2.0346 (12)	V2*b*—O3*b*	2.0766 (14)
V1*a*—O1*b*^{ii}	1.6955 (12)	V2*b*—O5*b*	1.6547 (14)
V1*a*—O6*b*^{iii}	1.9491 (13)	V2*b*—O7*b*	1.7383 (12)
V1*b*—O1*a*^{iv}	1.892 (2)	V3*a*—O2*a*	1.9755 (13)
V1*b*—O1*a*^{v}	1.961 (2)	V3*a*—O3*a*^{iv}	1.933 (2)
V1*b*—O4*a*	1.6501 (14)	V3*a*—O3*a*^{v}	1.936 (2)
V1*b*—O6*a*	1.9731 (14)	V3*a*—O6*a*	1.6510 (14)
V1*b*—O1*b*	2.2587 (14)	V3*a*—O7*a*	1.9464 (13)
V1*b*—O5*b*^{iii}	1.9590 (14)	V3*a*—O3*b*	2.2119 (15)
V2*a*—O2*a*^{i}	1.9141 (14)	V3*b*—O3*a*	2.2127 (15)
V2*a*—O2*a*^{ii}	1.9169 (14)	V3*b*—O2*b*	1.9589 (12)
V2*a*—O3*a*	2.0763 (14)	V3*b*—O3*b*^{i}	1.9317 (15)
V2*a*—O5*a*	1.6545 (14)	V3*b*—O3*b*^{ii}	1.9351 (15)
V2*a*—O7*a*	1.7580 (12)	V3*b*—O6*b*	1.6635 (14)
V2*a*—O7*b*	2.2659 (14)	V3*b*—O7*b*	1.9690 (13)

Symmetry codes: (i) $x, -y, z-\frac{1}{2}$; (ii) $x, 1-y, z-\frac{1}{2}$; (iii) $x-1, y, z$; (iv) $x, -y, \frac{1}{2}+z$; (v) $x, 1-y, \frac{1}{2}+z$.

3. Refinements

In the following discussion, atoms are denoted by *Xna* (*e.g.* V2*a*) following Kawada *et al.* (1978); *Xnb* (*e.g.* V2*b*) is the centrosymmetrically related atom in *C*2/*m*. For refinements in non-centrosymmetric space groups, the origin was defined by fixing the *x* and *z* coordinates for one of the V atoms, V1*a*. While this is not the best procedure today, this method has to be employed when using the *DUPALS* (Lundgren, 1983) and *JANA*2000 (Petříček & Dušek, 2000) software.

3.1. Stoe diffractometer data

The starting structure for the refinement of the Stoe data was taken from Kawada *et al.* (1978); refinements were made using *DUPALS* (Lundgren, 1983). The function minimized was $\Sigma w(F_o^2 - F_c^2)^2$ with $w = 1/\sigma^2(F^2)$, where $\sigma(F^2)$ was estimated from counting statistics and the scatter of the standard reflections.

Refinement in space group $P2_1/a$ (Kawada *et al.*, 1978) converged with a weighted *R* value on F^2 of *ca* 16%. However, the clear appearance of 0*k*0 reflections with $k \neq 2n$, for $k = \pm 1, \pm 3, +5$ and $+7$, showed that no twofold screw axis existed. On the other hand, the absence condition for *h*0*l*, $h \neq 2n$ reflections holds well; the space groups *P*2/*a* and *Pa* were thus tested. Since *P*2/*a* also gave a final $wR(F^2)$ value of *ca* 16%, the non-centrosymmetric *Pa* seemed the more appropriate choice.

Clear evidence of structural disorder was soon found in the form of large residual peaks in the difference-Fourier maps, especially around the V1*a* and V1*b* atoms in the single layer. Different disorder models were tested for V1*a* and V1*b*, with partially occupied sites on either side of the *a*-glide plane, but led to no significant decrease in $wR(F^2)$. Residuals in the difference electron-density map at the V1*a* and V1*b* sites indicated that a second-rank tensor was insufficient to describe the thermal displacement of these atoms. However, the use of a third-rank γ_{ijk} tensor to describe the displacement of V1*a* and V1*b* led to a decrease in $wR(F^2)$ from 7.4 to 5.8%. Extinction is a serious problem for V_6O_{13} at room temperature; this was considerably lower at 95 K, probably as a result of increased mosaicity after the crystal passed through the phase transition. A type I isotropic extinction parameter with a Gaussian distribution (Becker & Coppens, 1974) gave the best result. The most severely affected reflections were 003 and $00\bar{3}$, with $y = 0.75$. The signs of the *hkl* indices were reversed to test the absolute structure; an increase in $wR(F^2)$ from 5.8 to 6.2% showed the original assignment to be the correct one. The refinements were carried out using a dataset for which equivalent reflections under *m* symmetry were not averaged. It should be noted that the disorder tended to be limited to the single layer; after the final refinement cycle, $\Delta\rho_{min} = -1.80$ and $\Delta\rho_{max} = 2.26$ e Å^{-3} in the single layer, but $\Delta\rho_{min} = -0.85$ and $\Delta\rho_{max} = 1.05$ e Å^{-3} in the double layer. The final structure was transformed to the standard space group *Pc*.

3.2. Bruker diffractometer data

No extra reflections were observed other than those arising from the lowering of symmetry. Once again, 0*k*0 reflections with $k \neq 2n$ ruled out the space group $P2_1/c$, thus suggesting the space groups *P*2/*c* or *Pc*. The input structure was that refined from the Stoe diffractometer data; *JANA*2000 (Petříček & Dušek, 2000) was used for the structure refinement. The same structural information was obtained as for the Stoe data.

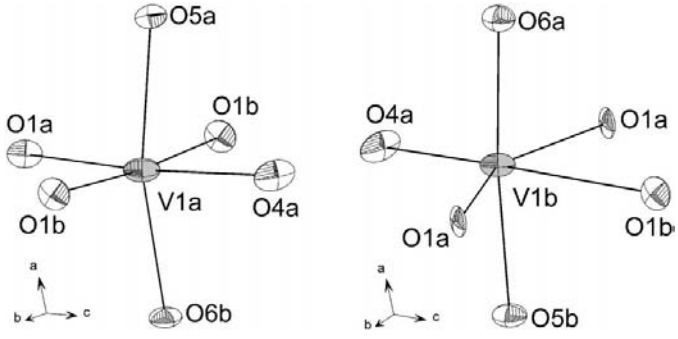

Figure 3
The oxygen coordination around the V1*a* and V1*b* atoms. Displacement ellipsoids are drawn at the 95% probability level.

4. Results and discussion

The DSC curve is shown in Fig. 1. The onset temperature of the phase transition was determined to be 153 K. Integration of the exothermic peak gave $\Delta H_{trans} = -1.98$ kJ mol^{-1}.

Final agreement factors *etc.* for both datasets are given in Table 1. The refined low-temperature structure from the Stoe diffractometer data is shown in Fig. 2. Atomic coordinates and equivalent isotropic displacement parameters have been deposited[1] and selected V—O distances are given in Table 2;

[1] Supplementary data for this paper are available from the IUCr electronic archives (Reference: BM5002). Services for accessing these data are described at the back of the journal.

Table 3
Selected bond-valence sums for V atoms in V_6O_{13} at room temperature and 95 K and for LiV_6O_{13}.

Structure	Atom	Bond-valence sum	Oxidation state % deviation	Atom	Bond-valence sum	Oxidation state % deviation	Atom	Bond-valence sum	Oxidation state % deviation
V_6O_{13} (298 K)	V1	4.262	4+ (7%)	V2	4.919	5+ (2%)	V3	4.616	5+ (8%)
V_6O_{13} (95 K)	V1*a*	4.645	5+ (7%)	V2*a*	4.865	5+ (3%)	V3*a*	4.320	4+ (8%)
	V1*b*	4.303	4+ (8%)	V2*b*	4.927	5+ (1%)	V3*b*	4.262	4+ (7%)
LiV_6O_{13} (298 K)	V11	4.150	4+ (4%)	V21	4.135	4+ (3%)	V31	4.323	4+ (8%)
	V12	4.168	4+ (4%)	V22	4.888	5+ (2%)	V32	4.665	5+ (7%)

all from the Stoe diffractometer data. Bond-valence sums were calculated using *VaList* (Wills & Brown, 1999) and are presented in Table 3.

At 95 K the *a* and *b* axes are slightly longer than at room temperature, while the *c* axis is shorter in the low-temperature structure. The β angle is virtually unchanged and the unit-cell volume at 95 K is 438.52 (5) Å^3 compared with 436.36 (6) Å^3 at room temperature. All room-temperature data are from Bergström *et al.* (1998*b*), where the same diffractometer and measurement technique has been used. The ratios between the cell parameters from the two measurements (Stoe data/Bruker data) are 1.0006, 1.0008 and 1.0007 for *a, b* and *c* respectively. This can be explained by the fact that the reflections used for refining cell parameters are centred on $K\alpha_1$ and $K\bar{\alpha}$ for the Stoe and Bruker data, respectively. Differences in cell parameters depending on measurement technique have been addressed elsewhere (Herbstein, 2000). Despite the differences in data quality and cell parameters, the same structural information is obtained from both data collections.

As reported by Kawada *et al.* (1978), all atoms move out of the mirror plane during the phase transition: however, our results differ in that no centre of symmetry is present. V1*a* moves out of the former mirror plane by as much as 0.21 (1) Å, while its near-equivalent V1*b* moves by only 0.06 (1) Å. The out-of-plane displacements for all other atoms are less than 0.035 Å, with the single-layer O atoms O1*a*, O1*b* and O4*a* exhibiting the largest shifts. The displacement ellipsoids of these atoms are somewhat elongated, even though the ellipsoids themselves are small. The four O atoms connecting the single and double layers (O5*a*, O5*b*, O6*a* and O6*b*) are all clearly affected by the large displacements of V1*a* and V1*b*. The displacement parameters for these O atoms are smaller than for those in the single layer, but slightly larger than for the O atoms in the double layer. The double-layer atoms barely move out of the mirror plane during the phase transition. The displacement ellipsoids and changes in bond distances are also small in the double layer. All VO_6 octahedra are distorted in the room-temperature structure, but even more so in the single layer of the low-temperature phase (Fig. 3). The largest difference in V1—O distances in the single-layer octahedron at room temperature is 0.30 Å, but this rises to 0.61 Å in the V1*b* octahedron at low temperature. Comparing room- and low-temperature bond distances for V1, it is clear that V1*b* has formed a distinct vanadyl bond with O4*a*, the bridging O atom between the VO_6 octahedra in the single layer. The V1*a*—O4*a* bond length has increased correspondingly. V1*a* has also formed a vanadyl bond, but in the *b* direction with O1*b*. The bond-valence calculations show that V1*a* has acquired more 5+ character than it has at room temperature. Correspondingly, both V3 atoms have developed 4+ character. It can be seen from Fig. 2(*a*) that the V1*a* and V3*b* octahedra share corners, as do the V1*b* and V3*a* octahedra. From bond-valence sums it can be concluded that charge transfer takes place between the V1 and V3 atoms during the phase transition.

That the structural changes appear mainly in the single layer is interesting. When lithium ions are inserted into the V_6O_{13} structure, they always bond to the single-layer O atoms for $x \leq 2$ (Bergström *et al.*, 1998*a*,*b*; Björk *et al.*, 2001). Furthermore, one of the V1 atoms forms a vanadyl bond, but to the O5 atom which bridges the single and double layers in the structure. The distortion in the V1 octahedron is significant; the vanadyl bond length is only 1.619 (1) Å, the opposite bond length is 2.757 (1) Å. The VO_6 octahedra would thus appear to be more strained in the single layer than in the double layer; given the opportunity, the V1 atom develops a vanadyl bond.

We wish to thank Mr Hilding Karlsson for his technical assistance throughout this work, which has been supported by The Swedish Science Council (VR) and The Swedish Energy Agency (STEM).

References

Becker, P. J. & Coppens, P. (1974). *Acta Cryst.* A**30**, 129–147.
Bergerhoff, G. (1996). *DIAMOND.* Visual Crystal Information System, Bonn, Germany.
Bergström, Ö., Gustafsson, T. & Thomas, J. O. (1998*a*). *Acta Cryst.* C**54**, 1204–1206.
Bergström, Ö., Gustafsson, T. & Thomas, J. O. (1998*b*). *Solid State Ion.* **110**, 179–186.
Björk, H., Lidin, S., Gustafsson, T. & Thomas, J. O. (2001). *Acta Cryst.* B**57**, 759–765.
Bruker (2001). *SMART* (Version 5.611) and *SAINT+* (Version 6.22). Bruker AXS Inc., Madison, Wisconsin, USA.
Chang, C. C., Kim, J. Y. & Kumta, P. N. (2000). *J. Power Sources*, **89**, 56–63.
Dernier, P. D. (1974). *Mater. Res. Bull.* **9**, 955–964.
Gover, R., Kanno, R., Mitchell, B., Hirano, A. & Kawamoto, Y. (2000). *J. Power Sources*, **90**, 82–88.
Herbstein, F. H. (2000). *Acta Cryst.* B**56**, 547–557.
Kachi, S., Takada, T. & Kosuge, K. (1963). *J. Phys. Soc. Jpn*, **18**, 1839–1840.
Kawada, I., Ishii, M., Saeki, M., Kimizuka, N., Nakano-Onoda, M. & Kato, K. (1978). *Acta Cryst.* B**34**, 1037–1039.

McCandlish, L. E., Stout, G. H. & Andrews, L. C. (1975). *Acta Cryst.* A**31**, 245–249.
Lehmann, M. S. & Larsen, F. K. (1974). *Acta Cryst.* A**30**, 580–584.
Lundgren, J.-O. (1983). *Crystallographic Computing Programs.* Report UUIC-B14-405. Institute of Chemistry, University of Uppsala, Sweden.
Ohzuku, T., Nakura, K. & Aoki, T. (1999). *Electrochim. Acta*, **45**, 151–160.
Petříček, V. & Dušek, M. (2000). *JANA*2000. *The Crystallographic Computing System*. Institute of Physics, Praha, Czech Republic.
Saeki, M., Kimizuka, N., Ishii, M., Kawada, I., Nakano, M., Ichinose, A. & Nakahira, M. (1973). *J. Cryst. Growth*, **18**, 101–102.
Stoe & Cie (1988). *DIF*4. Version 7. Stoe & Cie, Darmstadt, Germany.
Thackeray, M. M., David, W. I. F., Bruce, P. G. & Goodenough, J. B. (1983). *Mater. Res. Bull.* **18**, 461–472.
Wilhelmi, K. A., Waltersson, K. & Kihlborg, L. (1971). *Acta Chem. Scand.* **25**, 2675–2687.
Wills, A. S. & Brown, I. D. (1999). *VaList*, CEA, France.